Food Bioscience 64 (2025) 105918

Contents lists available at ScienceDirect

Food Bioscience

journal homepage: www.elsevier.com/locate/fbio

Characterization of the extracellular polymeric substances matrix of *Pseudomonas* biofilms formed at the air-liquid interface

Srinithi Muthuraman *, Steve Flint, Jon Palmer

Food Microbiology-Biofilm research, School of Food Technology and Natural Science, Massey University, 4412, Palmerston North, New Zealand

ARTICLE INFO

Keywords:
Psychrotrophic
eDNA
Stainless-steel
Enzymes
Polysaccharides

ABSTRACT

Pseudomonas are common psychotropic food spoilage organisms that affect the quality of aerobically chilled food products. Biofilm formation of these bacteria on food contact surfaces can provide a continuous contamination source, leading to food spoilage. *Pseudomonas* produce proteolytic and lipolytic enzymes which lead to organoleptic degradation of stored food products. The biofilm extracellular polymeric substances matrix (EPS) protects the bacterial cells from CIP (Cleaning-In-Place) chemicals and adverse conditions. Studies on the composition of the EPS matrix and the molecules present in the EPS matrix are limited. In this study, the EPS composition of mono-species biofilms of *Pseudomonas lundensis* and *Pseudomonas cedrina* on polystyrene and stainless-steel surfaces was characterized by chemical analysis and microscopical observations. The biofilms were allowed to grow on polystyrene and stainless-steel surfaces with half-strength TSB for 2 weeks at 30 °C and cold chain temperatures of 7 °C and 4 °C. The EPS was extracted by sonication and centrifugation and chemically analysed for cellulose, total polysaccharides, total proteins, and eDNA. *Pseudomonas* isolates in this study formed biofilms at the air-liquid interface. The formation of ring-like structures of cells was observed on the polystyrene surface. eDNA formed as a thread-like structure on a polystyrene surface while it formed channels on a stainless-steel surface. The amount of EPS varied at different temperatures. More EPS was formed at 4 °C than 30 °C. Flagellin, Clp protease, Arginine deiminase, and ATP-Binding Cassette (ABC) transporter substrate-binding proteins were the key proteins identified in the biofilm matrix of *P. lundensis*.

1. Introduction

Biofilms are aggregates of microbial cells attached to each other or the surface and embedded in a self-produced or acquired hydrated extracellular polymeric substances matrix (EPS). The matrix comprises polysaccharides, proteins, lipids, and extracellular DNA (eDNA) (Flemming & Wingender, 2010; Penesyan et al., 2021). Apart from these biomolecules, water is the major component of EPS. The EPS dries slowly, thus water in the EPS keeps the cells hydrated and protects them from desiccation (Or et al., 2007). EPS traps all the lysed components from the cells and each component in the EPS has its functionality such as adhesion, aggregation, water retention, nutrient source, and protective barrier (Karatan & Watnick, 2009).

Pseudomonas spp., forms biofilms in a wide range of environments such as dairy, poultry, meat processing, marine, and soil environments (Caldera & Franzetti, 2014; Jiang et al., 2011). Each species from the genus *Pseudomonas* produces diverse polysaccharides. *P. aeruginosa* is an alginate producer, while the soil pseudomonads such as *P. syringe* produce Levan in its extracellular matrix. Some other *Pseudomonas* are the cellulose producers (Li et al., 2010; Osman et al., 1986; Spiers et al., 2003). Apart from these capsular polymers, there are *Pel* and *Psl* polysaccharides involved in the biofilm formation. *Pel* is involved in the formation of pellicles observed in *Pseudomonas* that form air-liquid interface biofilms. *Psl* is also a non-capsular extracellular polysaccharide that is responsible for the attachment of cells to abiotic surfaces (Byrd et al., 2011; Coulon et al., 2010; Friedman & Kolter, 2004; Ma et al., 2009).

Pseudomonas spp., produces considerable amounts of extracellular proteins which include extracellular enzymes. Apart from enzymes, lectins (carbohydrate-binding proteins), DNA-binding proteins, glucan-binding proteins, and *Psl*-binding proteins are also found in *Pseudomonas*, *Streptococcus,* and *Glucanobacter* (Flemming & Wingender, 2010; Diggle et al., 2006). Proteins such as Cdr A, Lap A, and Lap D which are responsible for the adhesion to surfaces are also present in the biofilm matrix of *P. aeruginosa* and other *Pseudomonas* (Borlee et al., 2010; Hinsa et al., 2003).

* Corresponding author.
E-mail address: S.Muthuraman@massey.ac.nz (S. Muthuraman).

https://doi.org/10.1016/j.fbio.2025.105918
Received 26 November 2024; Received in revised form 9 January 2025; Accepted 13 January 2025
Available online 23 January 2025

Lipids in the matrix are mostly present either as lipopolysaccharides or lipoproteins. Rhamnolipids are identified in the biofilm matrix of many pseudomonads. Rhamnolipids can alter the surface properties by binding with the macromolecules either by hydrophilic or hydrophobic groups (Read et al., 1992; Boles et al., 2005).

Extracellular DNA in the matrix of *P. aeruginosa* is reported to be an intracellular connector(Otzen & Nielsen, 2008). This eDNA could be from the lysed cells or from cells that are actively excreting DNA into the biofilm matrix playing a major role in the structural properties of the biofilms (Otzen & Nielsen, 2008).

There is a lack of information on the composition of *Pseudomonas* biofilm matrices in terms of polysaccharides, proteins, and eDNA at different temperatures. This is important as temperature is one factor commonly used to reduce microbiological issues in the food industry. The source of eDNA within the biofilm structure is still to be resolved in terms of whether it is actively secreted into the biofilm structure or is present due to lysed cells (Wickramasinghe et al., 2020; Liu et al., 2023).

This present study aimed to analyse eDNA by sequencing the isolated eDNA and identifying the protein molecules present in the EPS along with their quantification. The polysaccharides quantified from previous research were soluble polysaccharides. This present study aimed to quantify cellulose (Mann & Wozniak, 2012) which is an insoluble polysaccharide identified in the biofilms of pseudomonads.

2. Materials and methods

2.1. Bacterial isolates and culture conditions

Strong biofilm-forming isolates at both 30 °C and 4 °C, 3SM (*P. lundensis*), and 20SM (*P. cedrina*) were chosen for this study. The isolates were obtained from raw milk collected from different dairy farms across New Zealand. Identifications were confirmed using PCR and 16S rRNA sequencing (Supplementary File 1). The stock cultures were prepared by streaking bacteria on the Tryptic soy agar (TSA, Difco™, Becton, Dickinson and Company, Franklin Lakes, New Jersey, USA) and incubating at 30 °C for 24 h. A single colony was picked and inoculated into a cryopreservation tube (Nalgene™, Merck, Darmstadt, Hesse, Germany) and stored at −80 °C for six months. Fresh, overnight cultures were prepared by streaking a stock culture on a TSA agar plate, incubating at 30 °C and inoculating a single colony in the Tryptic soy broth (TSB, Difco™, Becton, Dickinson and Company, Franklin Lakes, New Jersey, USA) overnight at 30 °C. This overnight culture was used for further experiments. The temperatures used for biofilm formation in this study were 30 °C, 7 °C, and 4 °C (cold storage and processing temperatures). Half-strength TSB was used as a medium as it encourages the biofilm formation of these dairy isolates (data not shown).

2.1.1. Biofilm formation on polystyrene surface

The biofilms were allowed to grow on 96 well microtiter plates. A cell suspension was diluted to obtain an OD_{600} (Absorbance at 600 nm) of 0.05 ± 0.015 (approximately 6 log CFU/mL) (Varioskan Lux 3020-1333, Thermo Fisher, Waltham, Massachusetts, USA) with half-strength TSB. Next, 200 μL of the adjusted inoculum was added to the wells of a 96-well microtiter plate (FALCON®, Corning Incorporated, Durham, USA). Two hundred microliters (200 μL) of half-strength TSB were added as a control. The plates were incubated at 30 °C, 7 °C, and 4 °C for two weeks. Spent media was discarded and fresh media was added every 72 h.

2.1.2. Biofilm formation on stainless-steel coupons

The stainless-steel coupons used in this study were 2.4 cm*2.4 cm and 1 mm thickness (316 with 2B finish). The coupons were passivated (with 50% nitric acid at 70 °C for 30 min) before being used for the biofilm formation assay. The coupons were sonicated for 15 min to remove any adhering cells and cleaned with ethanol and Tri Gene (Composition listed in supplementary file 1). The cleaned coupons were allowed to dry overnight and autoclaved at 121 °C for 15 min. The coupons were placed in the vials and filled with 4 mL of the inoculum to create an air-liquid interface on the surface of the coupons. The same culture concentration was maintained as the polystyrene surface. The vials were incubated at 30 °C, 7 °C, and 4 °C for two weeks. The coupons with 4 mL of half-strength TSB were used as a control. Spent media was replaced by fresh media every 72 h.

2.1.3. Planktonic cultures

The planktonic cultures (4 mL) were allowed to grow in the 15 mL tubes (Falcon®, Corning Incorporated, Durham, USA) for two weeks in half-strength TSB with the above-mentioned temperatures. One hundred microliters (100 μL) of culture were serially diluted and plated using a drop plate on TSA plates. The cell counts were expressed as logCFU/mL. The media was replaced for planktonic cultures same as biofilms.

2.2. Biofilm and planktonic growth

The biofilm and planktonic growth were monitored every 24 h by serial dilution with 0.85% sterile saline and plating on TSA plates. The cell counts were expressed as logCFU/cm^2 for biofilm cells and logCFU/mL for planktonic cells.

2.3. Microscopic observation

Polystyrene coupons of the same size as stainless-steel coupons and stainless-steel coupons were used for the microscopic observations. The coupons containing biofilms were removed and washed in sterile water three times to remove the media and loosely attached cells. The coupons were air-dried before staining. The coupons were observed under an epifluorescence microscope (Nikon Eclipse Ni-L, Nikon Instruments, Melville, New York, USA) with suitable filters. The images were captured by NIS-elements D software (Version 6.02.01(Build 1955), Nikon Instruments, Melville, New York, USA).

2.3.1. Acridine orange staining for cells

Acridine orange (Acridine Orange stain, BDH, London, England) 5 mg/mL was used to stain the biofilms. The dried biofilm containing coupons was stained with 100 μL of Acridine orange for 3 min. The coupons were washed and allowed to dry. With the Epi fluorescence microscope, the coupons were viewed with a TRITC filter (Excitation 532–550 nm and emission 574 nm). Acridine orange is membrane permeable, it stains the live cells with red-orange fluorescence (Sharma et al., 2020).

2.3.1.1. Filamentous cell formation. The colonies from the TSA plates were stabbed into semisolid agar (TSB + 0.2% agar) vials to assess the filamentous cell formation by restricted motility.

2.3.2. Calcofluor white staining for EPS

The dried coupons were stained with 1 drop of calcofluor white stain (Fluka® calcofluor white stain, Sigma Aldrich, Oakville, Ontario, Canada). The stain was washed with water after a minute and allowed to dry. The calcofluor white stained coupons were observed under an epifluorescence microscope with a DAPI filter (Excitation 340–360 nm and emission,410 nm). Calcofluor white binds to cellulose and chitin and emits blue and white fluorescence (Wang et al., 2023).

2.3.3. Pico green staining for eDNA

The dried coupons were stained with Pico green (Quant-iT™ Picogreen™, Thermofisher Scientific, Waltham, Massachusetts, USA) and kept in the dark for 5 min. The stained coupons were washed with sterile water and allowed to dry in a dark room. After drying, the coupons were observed under an epifluorescence microscope with a FITC filter (Excitation 465–490 nm and emission 512 nm). Pico green is membrane

impermeable and emits green fluorescence with dead cells and eDNA, and the live cells look darker (Ban & Kim, 2024).

2.4. Isolation of EPS

The EPS isolation protocol followed here is a modified protocol from Yang et al., 2019. After 2 weeks the plates were taken out from the incubator. The remaining media was removed by inverting the plates. The plates were washed more than thrice to completely remove the media and planktonic cells with sterile distilled water. After washing the plates were air dried. 200 μL of sterile distilled water was added to each well. The plates were sealed and sonicated (Bandelin Sonorex digitec, GmBH&Co, Berlin, Germany) for 30 min. After sonication, the contents in the wells were transferred into 1.5 mL Eppendorf tubes (Quality Scientific Plastics, Petaluma, California, USA). The EPS contents in the Eppendorf tubes were then centrifuged at 12000g for 5 min in a refrigerated centrifuge (Hettich, Mikro 220R, Gottingen, Germany). The supernatant was collected and filtered using a 0.2 μm syringe filter (Minisart, Sartorius, Gottingen, Germany). The supernatant was pooled into a 15 mL centrifuge tube (Falcon®, Corning Incorporated, Durham, North Carolina, USA) up to the volume of 3 mL. The centrifuge tubes were placed in the freeze dryer and the collected fraction was soluble EPS.

The stainless coupons were removed from the vials and washed with sterile water. Four of the coupons were filled with 5 mL of sterile water and sonicated for 30 min. After 30 min, the coupons were vortexed vigorously to completely dissolve the visible air-liquid interface biofilms. The contents were centrifuged at 12000*g* for 5min in a refrigerated centrifuge (4 °C) and filtered using a 0.2 μm syringe filter. 3 mL of the isolated EPS was filled in centrifuged tubes and placed in the freeze dryer.

After 2 weeks, the planktonic cultures were washed with sterile distilled water thrice by centrifugation at 3000*g* for 5 min at 25 °C to completely remove the TSB. Water (3 mL) was added to the cell pellets and mixed by vortex. The mixture was filled in 1 mL Eppendorf tubes and centrifuged at 12000*g* for 5 min at 4 °C. The supernatant collected was filtered through a 0.2 μm syringe filter. The collected cell-free supernatants (CFS) were placed in the freeze dryer.

2.5. Cellulose quantification

The extraction method defined above could only get the soluble components of EPS in the supernatant. As cellulose is an insoluble polymer the method was modified.

After 2 weeks of incubation, the plates were taken out from the incubator and washed to remove the media and planktonic cells. Then the wells were filled with 200 μL of water and sonicated for 30 min. The contents from the 32 wells were pooled into a centrifuge tube at a volume of 5 mL. Five millilitres of extraction buffer containing an 8:2:1 ratio of acetic acid, nitric acid, and distilled water was added and boiled for 30 min. The boiled contents were mixed by vortex and centrifuged at 10300*g* for 15 min at 30 °C. The supernatant was discarded, and the pellets were washed with 1 mL of water and 1 mL of acetone and left for drying overnight. After 24 h the pellet was diluted by 1 mL of sulfuric acid. Cellulose standards of 30, 50, 75, and 100 mg/mL were prepared. 0.2 g of anthrone was dissolved in 100 mL of sulfuric acid. 500 μL of anthrone was added to the wells in the 48 well plates. One hundred microliters of the samples and standards were added to the wells containing anthrone. The absorbance was measured at 620 nm, and the cellulose content was calculated as $\mu g/10^8$ cells (Wang et al., 2023).

2.6. Polysaccharide quantification

The phenol sulfuric acid assay described by Dubois et al., followed with modifications(DuBois et al., 1956)

Reagents	
5% Phenol	30 μL
98% Sulfuric acid	150 μL

Fifty microliters of the sample were added to a well in 96-well plates. One hundred fifty microlitres of (150 μL) of sulfuric acid were added, followed by 30 μL of phenol. The plates were shaken at room temperature for 5 min. Then, they were placed on hot plates at 90 °C for 5 min and cooled for 5 min. The absorbance was read at 490 nm. D-glucose was used as a standard (from 50 to 1000 μg/mL).

2.7. Protein quantification

The proteins in the EPS are quantified by the Lowry assay with the following reagents (Shen, 2023)

Reagent A

2% Na_2CO_3 in 0.1N NaOH	48 mL
1% Sodium potassium tartrate	1 mL
0.5% $CuSO_4.H_2O$	1 mL

Reagent B

Folin Ciocalteau.

Fifty microliters (50 μL) of sample and 1040 μL of Reagent A were added in an Eppendorf tube of 1.5 ml and left for 10 min. Reagent B (125 μL) was added and left for 30 min and the absorbance was read at 660 nm. The standard curve was prepared with Bovine Serum Albumin (BSA) from 50 to 1000 μg/mL. From the standard curve, proteins in the samples were quantified and expressed as $\mu g/10^8$ cells.

2.8. Protein identification (LC-MS)

The freeze-dried EPS was subjected to SDS-PAGE and the gels were stained with Coomassie brilliant blue. Protein bands of interest were excised from the gels. Pre-stained protein ladder used from the range of 10–250 kDa (PAGE regular Plus Prestained Protein Ladder, Thermofisher Scientific, Waltham, Massachusetts, USA). In-gel enzymatic digestion and protein identification (LC-MS) were performed by the Mass Spectrometry Centre, University of Auckland (New Zealand) (Goodman et al., 2018)

2.9. eDNA isolation and quantification

The freshly isolated biofilm EPS and Planktonic supernatant were used for eDNA quantification. Five microliters of the samples were added in the wells of 2% Agarose gels (E-gel® EX with SYBR Gold II, Invitrogen, Waltham, Massachusetts, USA) and visualized (E-Gel iBASE™, Invitrogen, Waltham, Massachusetts, USA). The samples were then cleaned and concentrated with a DNA clean and concentrate kit (ZYMO research, Irvine, California, USA) and quantified using Nanodrop (Thermofisher Scientific, Waltham, Massachusetts, USA). Partial 16S rDNA sequencing was done at Massey genomics using Big Dye Terminator v3.1the results were analysed by Chromas lite and BLAST gene bank. PCR amplification of 16S rDNA was used to confirm the identification of isolated eDNA using universal primers Bac27F(5′-AGAGTTTGATCCTGGCTCAG-3′) and 1492R(5′-TACGGYTACCTTGTTACGACTT-3′).

2.10. Data analysis

All experiments were performed with two or three biological replicates and more than three technical replicates. One-way variance analysis (ANOVA) was generated to evaluate significant differences among the variables using Tukey's test with a *p*-value below 0.05 considered as statistically significant. Data analysis was implemented

using SPSS statistical software(Version 29.0.2.0; IBM®, New York, United States).

3. Results

3.1. Visible biofilm formation

Pseudomonas form air-liquid interface biofilms (Figs. 1 and 2). The visible biofilm formation around the air-liquid interface of the coupons and wells was observed from 24 h. Compared to 30 °C, the biofilms formed at 7 °C and 4 °C showed thick visible biofilms in both stainless-steel and polystyrene surfaces. Pellicle formation was observed in both biofilm and planktonic cultures. The polystyrene surface started to show visible biofilms from 24h but for the stainless-steel surface, it was observed after 72 h, however, at the end of two weeks both surfaces showed thick visible biofilms at 7 °C and 4 °C (Figs. 1 and 2).

3.2. Biofilm and planktonic cell enumeration

The initial inoculum for biofilms and planktonic cultures was approximately 6 log CFU/ml. Biofilm and planktonic growth were monitored every 24 h by serial dilution and plating (Data shown in supplementary file 2). The cell counts of biofilms and planktonic cultures at the end of two weeks are listed in Tables 1 and 2.

The planktonic cells at 30 °C showed more cell counts compared to 4 °C and 7 °C, while the biofilm cells showed more cell numbers at 4 °C and 7 °C after two weeks. Notably, in the biofilm cells at 30 °C the cell counts fluctuated with response to media refreshment and this suggests dispersion of the cells was higher at 30 °C compared to 4 °C and 7 °C. These observations suggest that the biofilm formation of psychrotrophic *Pseudomonas* was encouraged at 7 °C and 4 °C. In both stainless-steel and polystyrene surfaces, 4 °C encouraged more visible biofilms and cell counts.

3.3. Microscopic observations

The biofilm and planktonic cells were observed under the microscope every 24 h to monitor growth and contamination. Acridine Orange and Calcofluor White dyes were used to view the biofilm cells, EPS, and biofilm architecture while Pico green was used to stain the eDNA. After 24 h incubation on a polystyrene surface, more cell aggregates were seen at 4 °C and 7 °C while at 30 °C few cell clusters were observed. On a stainless-steel surface, 30 °C got comparatively more cell clusters than the cold temperatures at 24 h. Cell counts also followed a similar trend (Supplementary File 1). The biofilm architecture was also different when comparing the polystyrene and stainless-steel surfaces. In the early stages, cells formed as a ringlike structure (Fig. 3A) on a polystyrene surface while no such patterns were observed on the stainless-steel surface. In the later days of incubation, the cell clusters(Fig. 3B) started growing around the ringlike structures. These observations suggest that surface characteristics influence the biofilm architecture.

Filamentous cells were observed within the biofilm structures. These cells were observed in the biofilms formed on both stainless-steel and polystyrene surfaces at 30 °C, 7 °C, and 4 °C (Fig. 4C and D). These filamentous cells were absent in the planktonic cultures. The EPS in the biofilms may restrict motility and cell division. This scenario was checked by growing the cells in a semi-solid medium (TSB with 0.2% agar) and observed under the epifluorescence microscope (Fig. 4A and B). There were long filaments seen in the cells grown in TSB semisolid media. This result suggests that restricting motility could be the reason for filamentous cell formation.

Pellicle formation of psychrotrophic pseudomonads was observed in this study. These isolates formed pellicles on both polystyrene and stainless-steel surfaces. Pellicle formation on planktonic cultures was observed after 24 h of incubation at all three temperatures in this study. Pellicles showed as tightly packed cells (Fig. 5) like biofilms while planktonic cells were not clustered. This observation also suggests that pellicle is a type of biofilm formed by *Pseudomonas*.

Pico green stain was used to view the eDNA in the biofilms. Pico green binds with nucleic acid and emits green fluorescence. Pico green is membrane impermeable and stains the dead and damaged cells. The dead cells from the biofilms are green in colour while the live cells look dark (Fig. 6A and B). On the polystyrene surface, there were thread-like structures (Fig. 6A) that connected the cell clusters while on the stainless-steel surface (Fig. 6B), thick grid-like channels were observed. These structures were eDNA strands that were stained by Pico green. eDNA in the biofilms were observed even at 24 h. This explains the role of eDNA even at the early stages of biofilm formation.

With calcofluor white, cells, and the EPS matrix can be viewed. At 4 °C and 7 °C, large aggregates were seen while at 30 °C aggregates, were smaller and sparsely distributed on both stainless-steel and polystyrene surfaces (Fig. 7B). At the end of two weeks, the biofilm cells were almost covered with the EPS matrix which can be seen with Calcofluor white staining at 4 °C (Fig. 7A). From the microscopic observations, psychrotrophic pseudomonads produce more EPS at 4 °C and 7 °C compared to 30 °C.

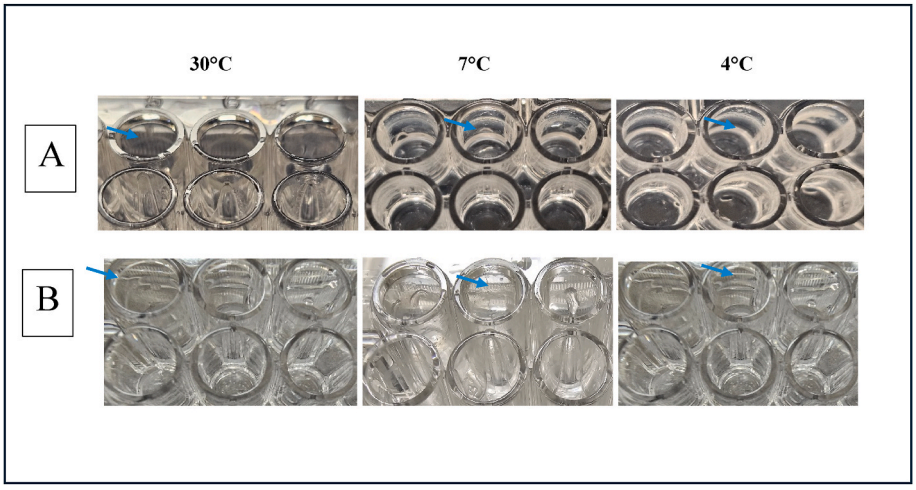

Fig. 1. Visible biofilms on polystyrene surface at 30 °C, 7 °C, and 4 °C at the end of two weeks. Blue arrows indicate the air-liquid interface biofilms. A represents the visible biofilms formed by isolate 3SM while B shows the visible biofilms formed by isolate 20SM.

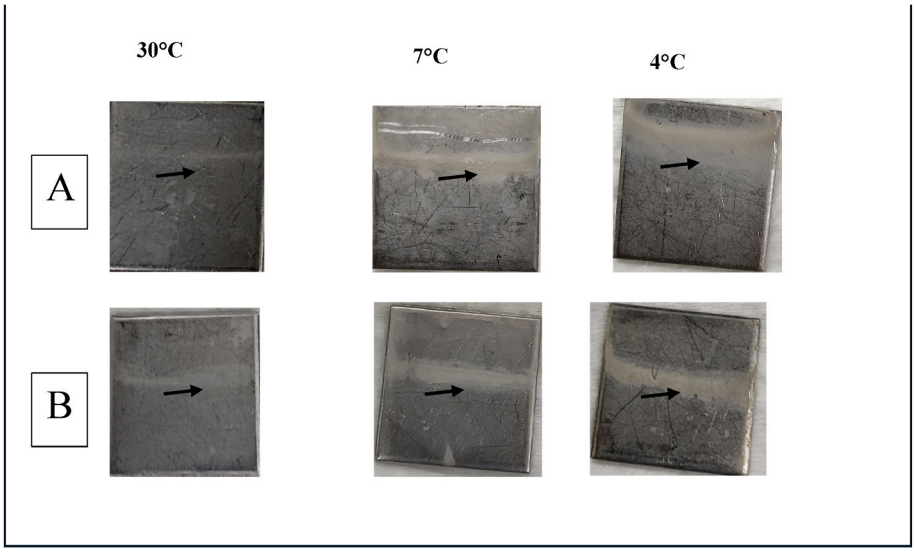

Fig. 2. Visible biofilm formation on stainless-steel surface at 30 °C, 7 °C, and 4 °C at the end of two weeks. Black arrows indicate the biofilm formation around the air-liquid interface. A shows the visible biofilms formed by isolate 3SM, while B shows the biofilms of isolate 20SM.

Table 1
Biofilm cell counts at the end of two weeks.

Bacterial Isolate	Surface	Cell counts (LogCFU/cm^2)		
		30 °C	7 °C	4 °C
3SM (*P. lundensis)*	Polystyrene surface	7.45 ± 0.10^{a}	8.37 ± 0.23^{ab}	8.95 ± 0.13^{b}
	Stainless-steel surface	6.05 ± 0.07^{a}	6.5 ± 0.05^{b}	7.63 ± 0.15^{c}
20SM (*P. cedrina)*	Polystyrene surface	7.03 ± 0.05^{a}	8.64 ± 0.06^{b}	8.84 ± 0.10^{b}
	Stainless-steel surface	6.88 ± 0.27^{a}	7.10 ± 0.10^{ab}	7.61 ± 0.23^{b}

Table 2
Planktonic cell counts at the end of two weeks.

Bacterial isolate	Cell counts (LogCFU/mL)		
	30 °C	7 °C	4 °C
3SM (*P.lundensis*	7.8 ± 0.13^{b}	7.56 ± 0.09^{a}	7.56 ± 0.10^{a}
20SM (*P.cedrina)*	7.80 ± 0.17^{b}	6.92 ± 0.07^{a}	6.86 ± 0.29a^{a}

Different letters above indicate significant differences ($p < 0.05$).

3.4. Quantification of cellulose

At all three growth temperatures, isolate 3SM produced more cellulose in the EPS than 20SM when it was allowed to grow on a stainless-steel surface. There was no significant($p > 0.05$) difference between the isolates for polystyrene EPS and planktonic CFS. Compared to 30 °C and 7 °C, 4 °C yielded significantly ($p < 0.05$) higher EPS in both the isolates (Fig. 8B). The isolate 3SM on stainless-steel yielded 85.445μg/10^8 cells at 30 °C, while at 4 °C the concentration was 417.04 which is about a 4.8-fold increase. On polystyrene surfaces, isolate 3SM yielded cellulose of 9.2 μg/10^8 cells at 30 °C, while at 4 °C it was 56.22 μg/10^8 cells, a 6.2-fold increase. Isolate 20SM also followed the same trend and showed around a 5.05-fold increase at 4 °C on stainless-steel and a 6.9-fold increase on a polystyrene surface. The temperature of 7 °C yielded more cellulose than 30 °C and comparatively less cellulose than 4 °C for both the isolates and on both surfaces. There was no significant ($p > 0.05$) difference between the temperatures for planktonic cellulose production.

3.5. Quantification of polysaccharides

When comparing the polysaccharide concentration there was no significant difference between the isolates in both the surfaces and planktonic CFS ($p > 0.05$). However, the biofilms grown at 4 °C yielded significantly ($p < 0.01$) higher concentrations than 30 °C and 7 °C in both polystyrene and stainless-steel surfaces (Fig. 9B). The isolate 3SM on a stainless-steel surface showed around 128.9 μg/10^8 cells at 30 °C, while at 4 °C it was 436.24 μg/10^8 cells which is about a 3.38-fold increase. For isolate 20SM at 30 °C the polysaccharide concentration was 91.02 μg/10^8 cells while the same isolate at 4 °C yielded about 449.9 μg/10^8 cells which is around a 4.9-fold increase. When the biofilms were allowed to form on a polystyrene surface, isolate 3SM showed a 6.5-fold increase at 4 °C and 20SM showed a 4.91-fold increase at 4 °C. This data

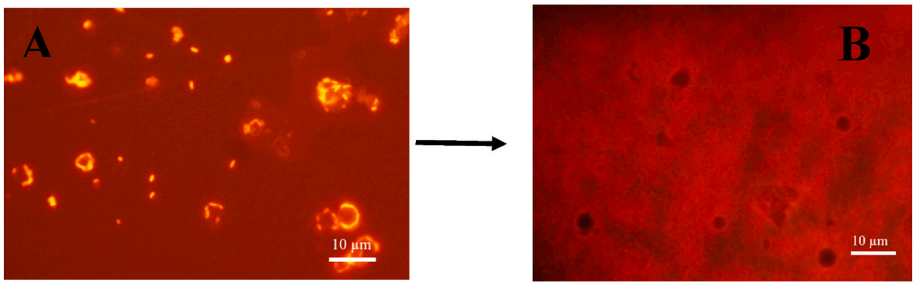

Fig. 3. (A) is from the biofilm of isolate 3SM at 24h which also shows the ringlike structures, while (B) is at 14th day which shows the cells grown around the ringlike structure(Scale bar 10 μm).

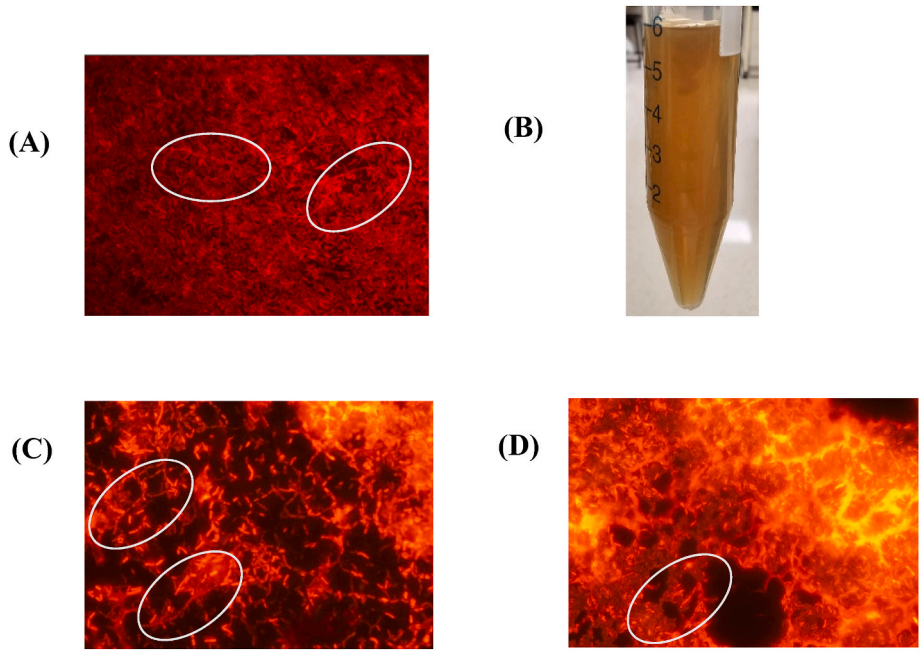

Fig. 4. Filamentous cells in the biofilm. (A) Filamentous cells grown in a semi-solid medium, (B) Semi-solid medium (TSB with 0.2% agar) with culture (C) and (D) Biofilms grown on stainless steel surface for the isolates 3SM and 20SM at 4 °C (Scale bar 10 μm).

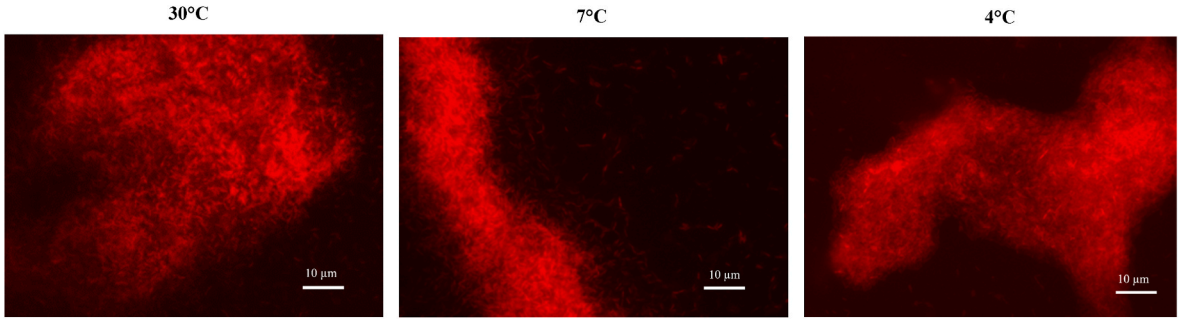

Fig. 5. Pellicles stained with Acridine Orange at 30 °C, 7 °C, and 4 °C from the planktonic cultures of the isolate 3SM(Scale bar 10 μm).

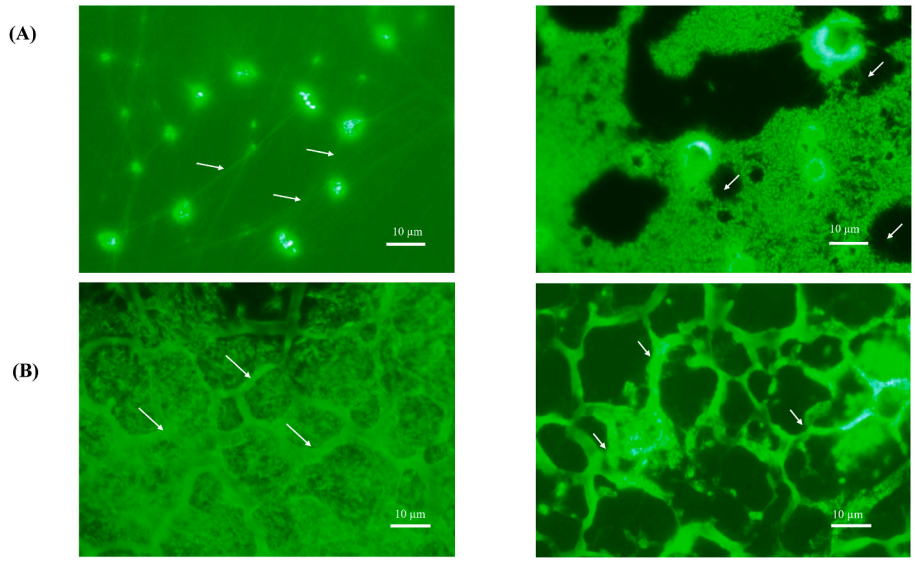

Fig. 6. eDNA structures in biofilms. (A) eDNA forms as thread-like structures on polystyrene surfaces,(B) eDNA channels on stainless-steel surface of isolate 3SM (Scalebar 10 μm).

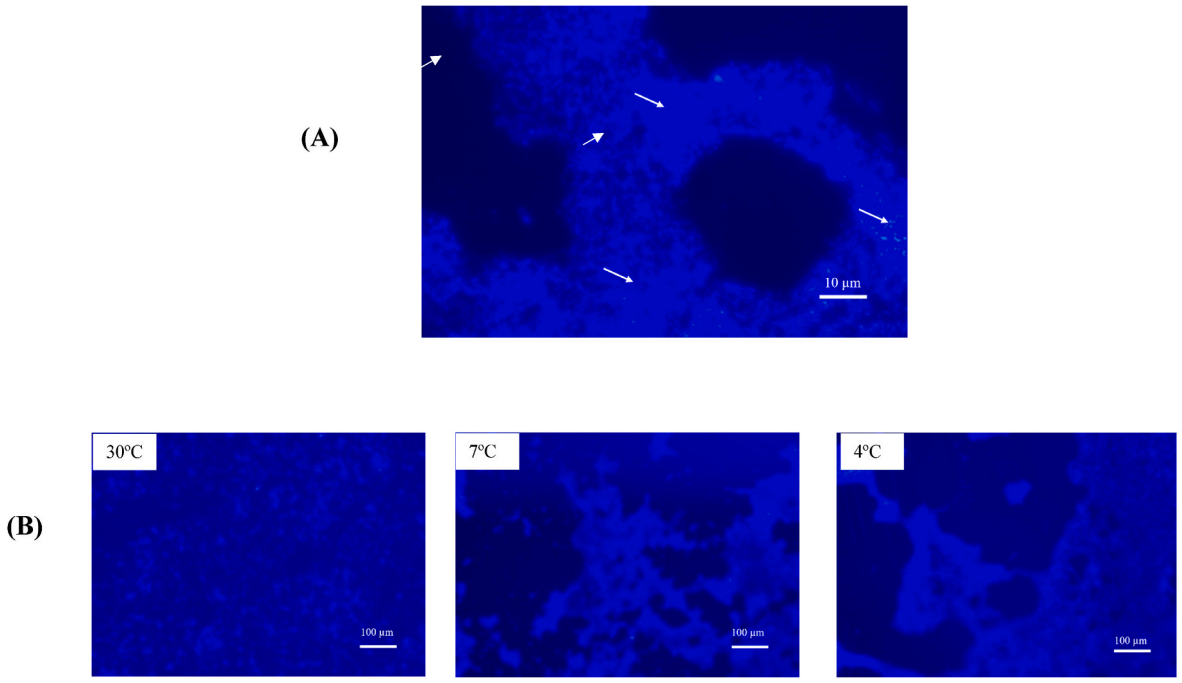

Fig. 7. (A) Isolate 3SM on a polystyrene surface at the end of two weeks, White arrows indicate the spots where EPS entirely covered the cells(Scale bar 10 µm). (B) Isolate 3SM on a polystyrene surface (Scale bar 100 µm).

suggests that the biofilm formation is increasing with a decrease in temperatures.

3.6. Quantification of proteins

The protein concentrations were compared and isolate 3SM produced significantly more proteins in their EPS at 4 °C and 7 °C on both stainless-steel ($p < 0.01$) and polystyrene ($p < 0.05$) surfaces. There was no significant ($p > 0.05$) difference between the proteins isolated from planktonic cell-free supernatant and the biofilms grown at 30 °C (Fig. 10B). There was a 6.22-fold increase in proteins observed for the biofilms of isolate 3SM grown on a stainless-steel surface at 4 °C at 697.945 µg/10^8 cells while at 30 °C total proteins were 112.55 µg/10^8 cells. Isolate 20SM on a stainless-steel surface showed a 4.93-fold increase in total proteins at 4 °C at 449.9 µg/10^8 cells while at 30 °C the total proteins were 91.02 µg/10^8 cells. Biofilms grown on polystyrene surfaces also produced more proteins at 4 °C than at 7 °C and 30 °C. Total proteins from the EPS at 30 °C were 22.63 µg/10^8 cells and increased by 5.04-fold at 4 °C at 111.7 µg/10^8 cells for isolate 3SM. The total proteins at 30 °C, 12.89 µg/10^8 cells, and there was a 2.41-fold increase observed at 4 °C at 29.33 µg/10^8 cells. There was also a notable quantity of proteins observed from the planktonic CFS. The total protein concentrations at 7 °C were higher than 30 °C and lower than 4 °C for both surfaces.

3.7. Quantification of eDNA

eDNA is a major component in biofilms. There was no significant ($p > 0.05$) difference in eDNA concentration between the isolates grown as biofilms on polystyrene and planktonic cultures. However, the polystyrene biofilms at 4 °C, produced significantly higher eDNA ($p < 0.05$) than at other temperatures. Isolate 3SM yielded significantly higher eDNA ($p < 0.01$) in its biofilms than isolate 20SM (Fig. 11). There was a 3.42-fold increase in eDNA to approximately 15.75 ng/10^8 cells observed in the biofilms on stainless-steel growing at 4 °C. The same isolate as a biofilm on a polystyrene surface showed a 5.28-fold increase in eDNA at 4 °C compared to other temperatures. Isolate 20SM showed a 2.14-fold increase in the eDNA to approximately 2.64 ng/10^8 cells at 4 °C on a stainless-steel surface. On a polystyrene surface, there was a 4.54-fold increase in eDNA observed at 4 °C (Fig. 11). The planktonic cultures showed eDNA concentrations of less than 1ng/10^8 cells for all three temperatures tested, which supports eDNA is a feature of biofilm characteristic. The higher concentrations of eDNA isolated from the stainless-steel biofilm EPS of isolate 3SM facilitated eDNA sequencing. The resulting sequence was not different from the genomic DNA. This suggests the observed difference between planktonic and biofilm cells is gene expression.

3.8. Protein identification

Proteins from the EPS were analysed by SDS-PAGE and Coomassie blue staining (Fig. 12). The bands were different between the two dairy isolates. Isolate 3SM showed bands at 250 and 130 kDa while for isolate 20SM the bands started from 75 kDa. Around 35 kDa molecular weight the isolate 20SM showed parallel bands while the isolate 3SM showed single bands. The bands from the biofilms grown at 30 °C were not clear compared to 7 °C and 4 °C which indicates the matrix overproduction at cold temperatures. More bands from isolate 3SM can be correlated with the total proteins that showed higher protein content than isolate 20SM. The planktonic CFS showed weaker bands and only the bands near 55 kDa were clear. The bands showing a molecular weight of approximately 55 kDa were present in both the isolates and in both biofilm EPS and the planktonic CFS (Fig. 12). However, LC-MS/MS revealed that the 55 kDa bands in isolate 3SM were flagellin and in 20SM it was Chaperonin GROEL. The proteins identified in the biofilms of isolate 3SM are listed in Table.

4. Discussion

The isolates in this study 3SM (*P. lundensis*) and 20SM (*P. cedrina*) formed air-liquid interface biofilms. Many studies have reported biofilm formation however, only a few studies discussed biofilm formation at the air-liquid interface and its impact on food industries. In the food processing environment, an air-liquid interface can be seen in partly

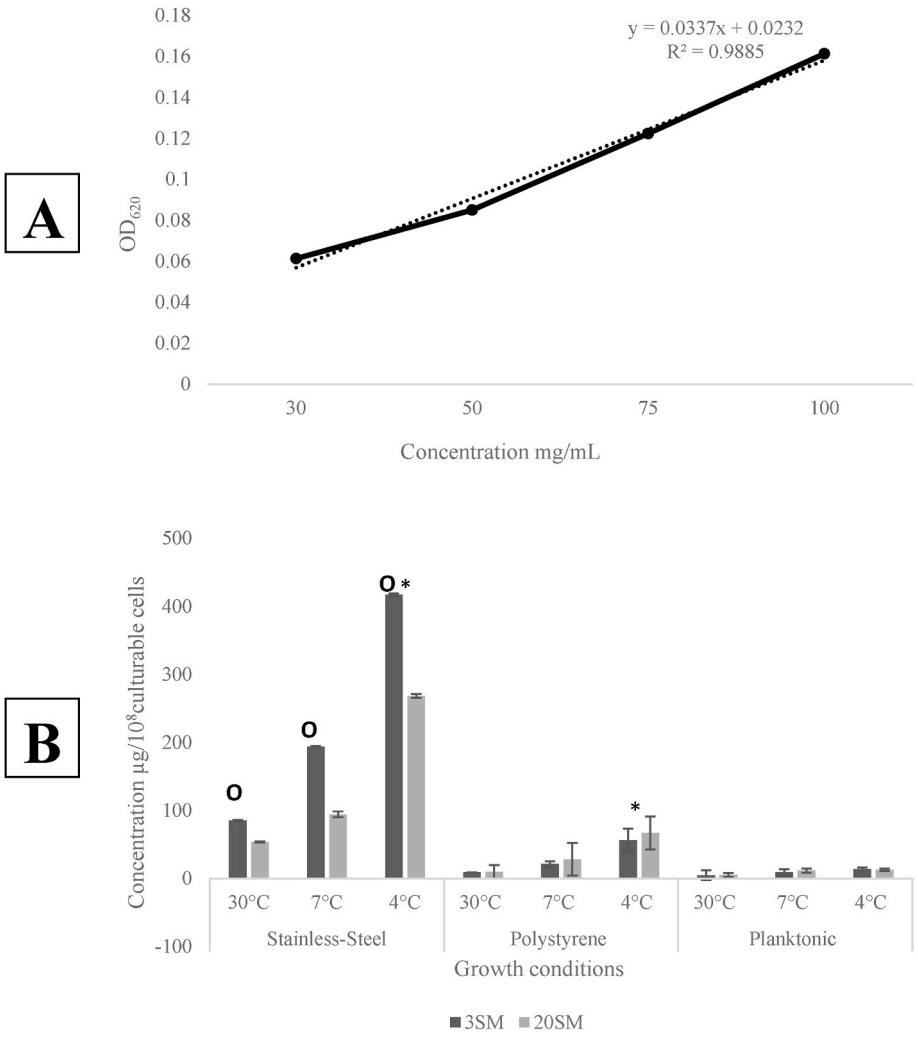

Fig. 8. Graph A shows the standard microcrystalline cellulose curve from 30 mg/mL to 100 mg/mL. Graph B shows the quantity of cellulose isolated from the EPS of biofilms and the planktonic cell-free supernatant. Results are expressed in mean ± standard deviation. "*" indicates the significant difference between the temperatures while "O" indicates the difference between the isolates.

filled equipment, storage, piping systems, and residual liquid after cleaning (Jha et al., 2020). The air-liquid interface biofilms of *B. cereus* have a log higher cell counts (logCFU/cm^2)than the submerged stainless-steel coupons. The oxygen availability causes aero taxis of the cells towards oxygen (Wijman et al., 2007). However, in the present study, isolates formed a thick air-liquid interface at 7 °C and 4 °C compared to 30 °C. A study on the influence of temperature on biofilm formation in wastewater biofilms showed that at lower temperatures, dissolved oxygen was higher in the wastewater which in turn altered the metabolites and encouraged the production of polysaccharides with C=O and O=C-O which enhanced the resistance of the biofilms (Li et al., 2022).

The planktonic growth of *Pseudomonas* sp.AU10 observed at 30 °C and 4 °C shows that this psychrotrophic *Pseudomonas* showed more logCFU/ml of cells at 30 °C than at 4 °C. The temperature downshift is due to growth arrest by mesophiles and psychrophiles under cold temperatures (García-Laviña et al., 2019). In this present study, the planktonic cells showed more logCFU/ml at 30 °C compared to 7 °C and 4 °C. However, the biofilm cell counts were higher at 7 °C and 4 °C. In a previous study, comparing the biofilm formation of *P. aeruginosa* at four different temperatures(20, 25, 30, and 37 °C), the lowest showed more biofilms and low dispersion (Kim et al., 2020). *P. lundensis* isolated from meat source showed higher crystal violet values(biofilm) and protease activity at 4 °C compared with 10 and 30 °C. This indicates the role of biofilm formation in food spoilage and contamination (Liu et al., 2015).

In the present study, biofilm cells on both polystyrene and stainless-steel surfaces were observed with acridine orange staining revealing a biofilm architecture that differed depending on the surface. On the polystyrene surface, the formation of ringlike structures was observed while on the stainless-steel surface, the cells covered the surface with uneven clusters. Similar observations from a study comparing the air-liquid interface of *P. fluorescens* Pf1 on different surfaces such as polypropylene, glass, and stainless-steel showed, the formation of weblike structures on polypropylene while on stainless-steel and glass, heterogeneous distribution was observed. Polypropylene is a hydrophobic material however, the author concludes, based on existing literature it is difficult to emphasize hydrophobicity is the major reason for biofilm architecture (Jha et al., 2020). In the present study, filamentous cells were seen with acridine orange staining with both the surfaces and all the temperature conditions but were absent in planktonic cells. Bacteria produce filamentous cells as survival mechanisms against stressful environments (Khan et al., 2022). In biofilms the filamentous cell morphology aids in the adhesion on biotic or abiotic surfaces (Khan et al., 2022). However, not all the cells formed filaments and stress is not the reason for filamentous cell formation in the present study. Some of the cells undergo morphogenesis via cell-cell communication and form filamentous cells and interconnect bacterial clusters. (Anbumani et al., 2021).

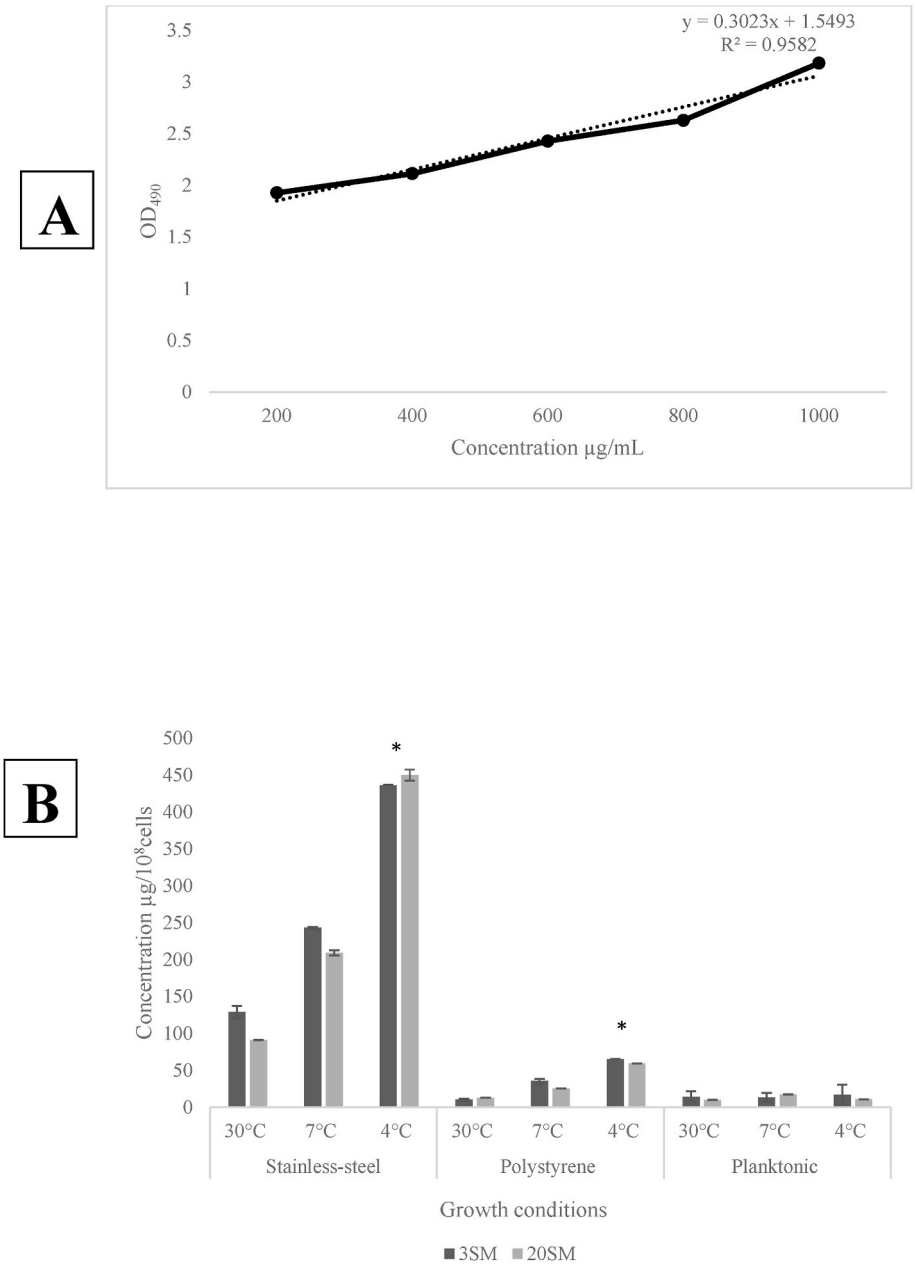

Fig. 9. Graph A shows the standard curve for D-Glucose from 200 µg/mL to 1 mg/mL. Graph B shows the total polysaccharides concentration from the biofilm EPS and Planktonic cell-free supernatant. Results are expressed in mean ± standard deviation. "*" indicates the significant difference between the temperatures.

Longitudinal cross-packed cells were observed in the pellicles formed by *P. alkylphenolica* KL28 and the controlled growth of pellicle cells accumulate extracellular polymeric substances (Song et al., 2018). The thin layer observed in between the cells indicates its role in pellicle floatation. In this present study both the isolates formed pellicles with tightly packed cells. This indicates the role of pellicle formation in these psychrotrophic pseudomonads.

Calcofluor white stains the cellulosic biomass in the biofilms, and the biofilms of *S. aureus* stained with calcofluor white showed similar structures (García-Salinas et al., 2018). More blue fluorescence was observed for the biofilms grown at 4 °C, compared to 15 °C and 25 °C suggesting more exopolysaccharide secretion at cold temperatures by *Pseudomonas* (Liu et al., 2023). This present study also highlighted similar observations where at 30 °C the biofilm formation was with small and unevenly distributed cell clusters while at 4 °C and 7 °C larger aggregates were observed. Compared with cell counts, the psychrotrophic *Pseudomonas* produce significantly ($p < 0.05$) higher exopolysaccharides with cold temperatures which is confirmed with quantification of EPS components.

eDNA is a major component in the EPS matrix. eDNA can possess different structures from amorphous mass to filamentous fibres and grid-like structures. The biofilms of *Xanthomonas citri* subsp *citri* formed on a glass surface showed amorphous eDNA structures in the early stages of biofilm formation and long fibers after 72 h of incubation (Sena-Vélez et al., 2016). Similar kinds of fibres were present in the polystyrene biofilm. From 24 h the fibre structure is established and the short amorphous structures around the cell clusters are newly formed. The biofilms formed on stainless-steel surfaces showed grid-like structures. Similar grid-like structures are observed in the biofilms of *P. aeruginosa* and thick rope-like channels are observed in the biofilms of *Haemophillus influenzae* (Allesen-Holm et al., 2006; Böckelmann et al., 2006). Thus, surface characteristics influence the components of EPS and biofilm architectures.

The dairy isolates in this study showed differences in their matrix

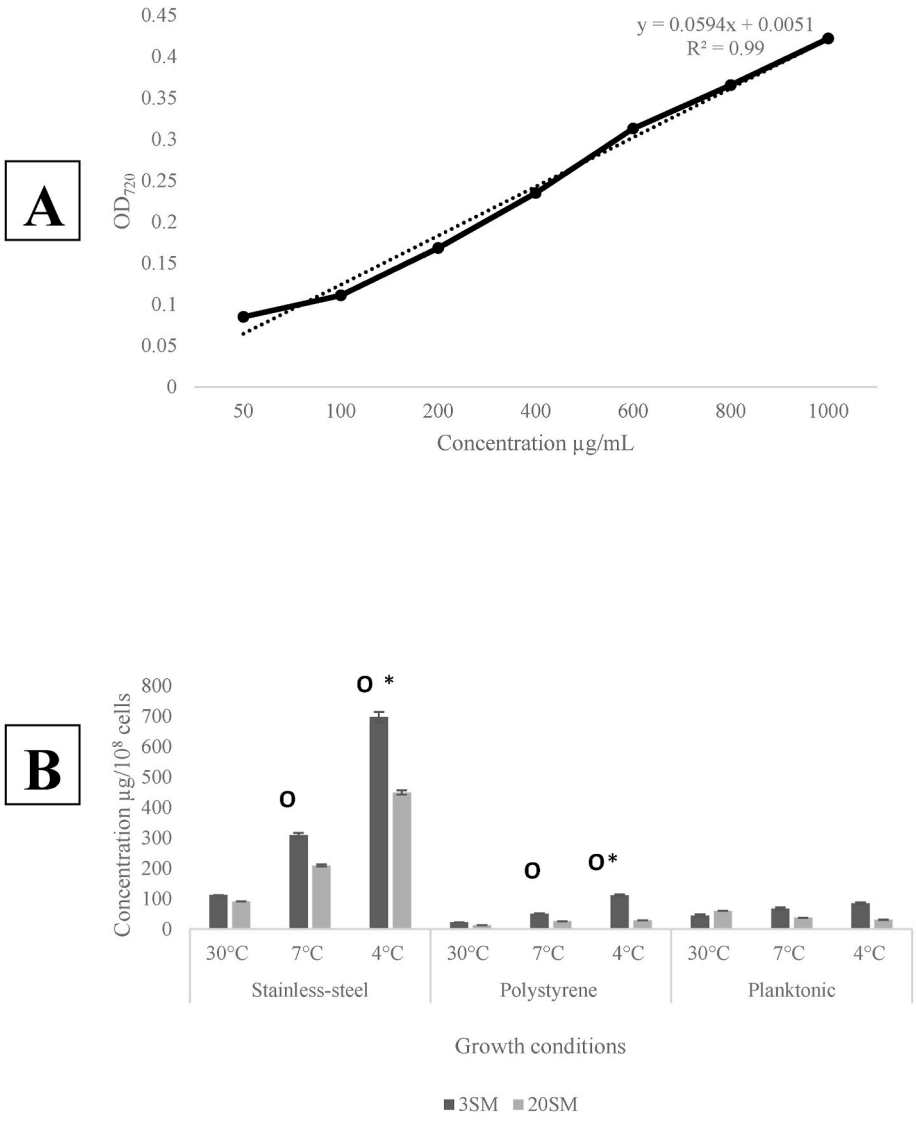

Fig. 10. Graph A shows the standard curve for Bovine serum albumin from 50 µg/ml to 1 mg/ml. Graph B shows the total protein concentrations from the biofilm EPS formed on stainless-steel and polystyrene surfaces and the proteins from planktonic CFS. The results are expressed in mean ± standard deviation. "*" represents the significant difference between the temperatures while "O" represents the significant difference between the isolates.

composition. The isolate 3SM showed significantly higher cellulose and proteins compared to the isolate 20SM. These key differences may play a major role in their biofilm integrity and strength. However, both the isolates showed similar quantities of soluble polysaccharides in their EPS matrix. The isolate 3SM produced more proteins to total polysaccharides in the EPS matrix and a higher amount of cellulose. Even though these isolates exhibited similar biofilm-forming abilities in terms of biomass and cell numbers (data not shown), the biofilm EPS matrix composition differed. In a recent study, even though there is a close taxonomic difference between *P. fragi* and *P. lundensis* the amounts of carbohydrates and proteins in the biofilms of these bacteria were different (Wickramasinghe et al., 2020). The information on the EPS matrix composition is essential in designing an eradication strategy. The cleaning agent needs to successfully degrade the EPS matrix especially the exopolysaccharides, proteins, and eDNA (Wang et al., 2023).

In the present study, flagellin was identified in the EPS matrix of isolate 3SM. The flagellin homologous proteins in the *Vibrio vulnicus* biofilms do not participate in the construction of flagellar filaments but are involved in strengthening the biofilm matrix (Jung et al., 2019).

In the present study, the same 55 kDa proteins were present in planktonic CFS and biofilm EPS. However, the functions of the flagellin protein might be different between biofilm and planktonic cells. The 55 kDa band from isolate 20SM was identified as Chaperonin GroEL. Heat shock in *E. coli* induced a three-fold increase in GroEL indicating the chaperonin function under stress (Wagner et al., 2024). Another interesting molecule identified in the EPS of isolate 3SM was the ATP-dependent Clp protease ATP binding subunit. The ClpP are present in the biofilms of *X. oryzae* and are responsible for pathogenicity, biofilm production, swimming ability, and EPS production (Ni et al., 2021).

The Arginine deiminase system was identified in the present study in isolate 3SM. This system is found in oral biofilms of *Streptococcus mutans*, where it catabolizes the L-arginine which can inhibit the water-insoluble exopolysaccharide production (Huang et al., 2017).

The ABC transport molecules identified in the present study in isolate 3SM (Table 3), are involved in the translocation of diverse substrates across the membranes (Thomas & Tampé, 2020). However, the present study only focussed on the soluble EPS and it needs more research in terms of bound EPS.

When grown on a stainless-steel surface the isolate 3SM showed significantly higher eDNA than the isolate 20SM, notably at 4 °C. In published work, *P. lundensis* shows significantly high levels of eDNA at cold temperatures, and cellular disruption and cell death at cold

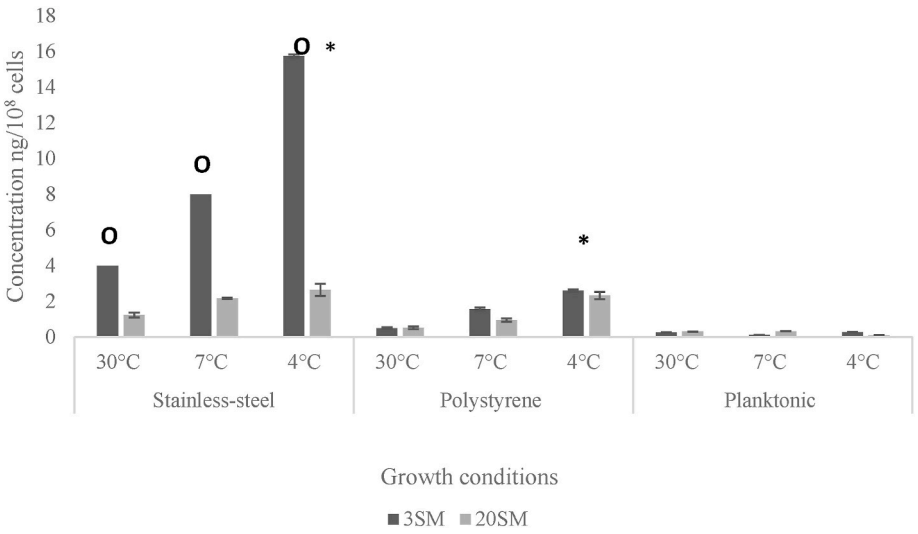

Fig. 11. The graph here represents the concentration of eDNA present in the biofilms grown on stainless steel and polystyrene surfaces and the planktonic cell-free supernatant. The results were expressed in mean ± standard deviation. "*" represents the significant difference between the temperatures while "O" represents the significant difference between the isolates.

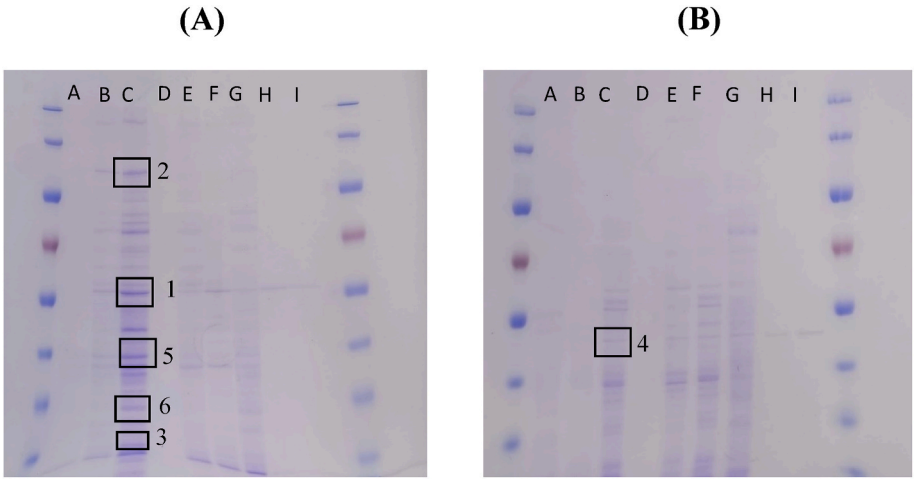

Fig. 12. A represents the proteins isolated from Gel electrophoresis of isolate 3SM while "B" shows the bands from isolate 20SM. The alphabets in the gels represent as follows.
A- 30 °C stainless-steel EPS.
B- 7 °C stainless-steel EPS.
C- 4 °C stainless-steel EPS.
D- 30 °C polystyrene EPS.
E– 7 °C polystyrene EPS.
F- 4 °C polystyrene EPS.
G- 30 °C planktonic CFS.
H- 7 °C planktonic CFS.
I- 4 °C planktonic CFS.
(Protein ladder range – 10–250 kDa). The bands excised for LC/MS/MS are marked with numbers 1 to 6.

temperatures could be the reason for higher eDNA production (Wickramasinghe et al., 2020). Bacterial cell lysis is the major mechanism behind the eDNA release in some gram-positive and negative pathogens however some bacteria such as *E. faecalis* and *Neisseria gonorrhoea* actively secrete eDNA. In *N. gonorrhoea* biofilm, type IV pili release large quantities of eDNA (Campoccia et al., 2021). The 16s rRNA sequencing of the isolated eDNA confirmed that it is not different from genomic DNA (Supplementary file 5), confirming that eDNA must be released due to lysis. However, the secretion system of eDNA release of these organisms needs to be studied.

Stainless-steel and polystyrene surfaces are commonly found in food processing environments. Polystyrene is mostly used for packaging, while stainless-steel is a food-contact surface (Paz-Méndez et al., 2017). In this study, the isolates formed strong biofilms on both surfaces at 4 °C and 7 °C. The stainless-steel surface encouraged more EPS production with approximately 7.5 log CFU/cm^2. This suggests that with fewer cells, these isolates can produce more EPS.

5. Conclusion

Food spoilage by psychrotrophic pseudomonads is common in dairy and meat processing environments. Temperature is a key factor affecting

Table 3
Proteins identified from the biofilms of 3SM and 20SM grown at 4 °C on stainless-steel coupons.

No	Molecular weight (kDa)	Protein	Isolate
1	55	Flagellin	3SM
2	130	ATP-dependent Clp protease ATP binding subunit	3SM
3	10	ABC transporter substrate-binding proteins	3SM
4	55	Chaperonin GROEL	20SM
5	35	Arginine deiminase	3SM
6	25	Branched chain-amino acid ABC transporter substrate-binding proteins	3SM

the biofilm formation of psychrotrophic pseudomonads. Microscopical observations, matrix quantification, and cell count suggested that cold temperatures of 4 °C and 7 °C yielded higher cells and EPS than the biofilms formed at 30 °C. Surface characteristics are also an important factor influencing these pseudomonads' biofilm architecture. Knowledge on what are all the key components present in the EPS matrix is important for designing elimination strategies. This study attempted to find the protein molecules present in the EPS matrix. This study highlighted the compositional differences in the EPS formed by two dairy isolates even though both formed strong biofilms under cold temperatures. However, the interaction between the EPS components needs to be studied. Overall, this study emphasized the biofilm formation of psychrotrophic pseudomonads under cold temperatures.

CRediT authorship contribution statement

Srinithi Muthuraman: Writing – original draft, Methodology, Investigation, Formal analysis, Conceptualization. **Steve Flint:** Writing – review & editing, Validation, Supervision, Conceptualization. **Jon Palmer:** Writing – review & editing, Validation, Supervision, Conceptualization.

Declaration of competing interest

The authors declare that they have no known competing financial interests or personal relationships that could have appeared to influence the work reported in this paper.

Appendix A. Supplementary data

Supplementary data to this article can be found online at https://doi.org/10.1016/j.fbio.2025.105918.

Data availability

Data will be made available on request.

References

Allesen-Holm, M., Barken, K. B., Yang, L., Klausen, M., Webb, J. S., Kjelleberg, S., Molin, S., Givskov, M., & Tolker-Nielsen, T. (2006). A characterization of DNA release in *Pseudomonas aeruginosa* cultures and biofilms. *Molecular Microbiology, 59*(4), 1114–1128. https://doi.org/10.1111/j.1365-2958.2005.05008.x

Anbumani, S., Da Silva, A. M., Carvalho, I. G. B., Fischer, E. R., De Souza E Silva, M., Von Zuben, A. A. G., Carvalho, H. F., De Souza, A. A., Janissen, R., & Cotta, M. A. (2021). Controlled spatial organization of bacterial growth reveals key role of cell filamentation preceding *Xylella fastidiosa* biofilm formation. *Npj Biofilms and Microbiomes, 7*(1), 86. https://doi.org/10.1038/s41522-021-00258-9

Ban, E., & Kim, A. (2024). PicoGreen assay for nucleic acid quantification—applications, challenges, and solutions. *Analytical Biochemistry, 692*, Article 115577. https://doi.org/10.1016/j.ab.2024.115577

Böckelmann, U., Janke, A., Kuhn, R., Neu, T. R., Wecke, J., Lawrence, J. R., & Szewzyk, U. (2006). Bacterial extracellular DNA forming a defined network-like structure. *FEMS Microbiology Letters, 262*(1), 31–38. https://doi.org/10.1111/j.1574-6968.2006.00361.x

Boles, B. R., Thoendel, M., & Singh, P. K. (2005). Rhamnolipids mediate detachment of *Pseudomonas aeruginosa* from biofilms. *Molecular Microbiology, 57*(5), 1210–1223. https://doi.org/10.1111/j.1365-2958.2005.04743.x

Borlee, B. R., Goldman, A. D., Murakami, K., Samudrala, R., Wozniak, D. J., & Parsek, M. R. (2010). *Pseudomonas aeruginosa* uses a cyclic-di-GMP-regulated adhesin to reinforce the biofilm extracellular matrix. *Molecular Microbiology, 75*(4), 827–842. https://doi.org/10.1111/j.1365-2958.2009.06991.x

Byrd, M. S., Pang, B., Hong, W., Waligora, E. A., Juneau, R. A., Armbruster, C. E., … Swords, W. E. (2011). Direct evaluation of *Pseudomonas aeruginosa* biofilm mediators in a chronic infection model. *Infection and Immunity, 79*(8), 3087–3095. https://doi.org/10.1128/iai.00057-11

Caldera, L., & Franzetti, L. (2014). Effect of storage temperature on the microbial composition of ready-to-use vegetables. *Current Microbiology, 68*, 133–139. https://doi.org/10.1007/s00284-013-0430-6

Campoccia, D., Montanaro, L., & Arciola, C. R. (2021). Tracing the origins of extracellular DNA in bacterial biofilms: Story of death and predation to community benefit. *Biofouling, 37*(9–10), 1022–1039. https://doi.org/10.1080/08927014.2021.2002987

Coulon, C., Vinogradov, E., Filloux, A., & Sadovskaya, I. (2010). Chemical analysis of cellular and extracellular carbohydrates of a biofilm-forming strain *Pseudomonas aeruginosa* PA14. *PLoS One, 5*(12), Article e14220. https://doi.org/10.1371/journal.pone.0014220

Diggle, S. P., Stacey, R. E., Dodd, C., Cámara, M., Williams, P., & Winzer, K. (2006). The galactophilic lectin, LecA, contributes to biofilm development in *Pseudomonas aeruginosa*. *Environmental Microbiology, 8*(6), 1095–1104. https://doi.org/10.1111/j.1462-2920.2006.001001.x

DuBois, M., Gilles, K. A., Hamilton, J. K., Rebers, P. A., & Smith, F. (1956). Colorimetric method for determination of sugars and related substances. *Analytical Chemistry, 28*(3), 350–356. https://doi.org/10.1021/ac60111a017

Flemming, H.-C., & Wingender, J. (2010). The biofilm matrix. *Nature Reviews Microbiology, 8*(9), 623–633. https://doi.org/10.1038/nrmicro2415

Friedman, L., & Kolter, R. (2004). *Two genetic loci produce distinct carbohydrate-rich structural components of the Pseudomonas aeruginosa biofilm matrix*. https://doi.org/10.1128/JB.186.14.4457-4465.2004

García-Laviña, C. X., Castro-Sowinski, S., & Ramón, A. (2019). Reference genes for real-time RT-PCR expression studies in Antarctic *Pseudomonas* exposed to different temperature conditions. *Extremophiles, 23*(5), 625–633. https://doi.org/10.1007/s00792-019-01109-4

García-Salinas, S., Elizondo-Castillo, H., Arruebo, M., Mendoza, G., & Irusta, S. (2018). Evaluation of the antimicrobial activity and cytotoxicity of different components of natural origin present in essential oils. *Molecules, 23*(6), 1399. https://doi.org/10.3390/molecules23061399

Goodman, J. K., Zampronio, C. G., Jones, A. M. E., & Hernandez-Fernaud, J. R. (2018). Updates of the in-gel digestion method for protein analysis by mass Spectrometry. *Proteomics, 18*(23), Article 1800236. https://doi.org/10.1002/pmic.201800236

Hinsa, S. M., Espinosa-Urgel, M., Ramos, J. L., & O'Toole, G. A. (2003). The transition from reversible to irreversible attachment during biofilm formation by *Pseudomonas fluorescens* WCS365 requires an ABC transporter and a large, secreted protein. *Molecular Microbiology, 49*(4), 905–918. https://doi.org/10.1046/j.1365-2958.2003.03615.x

Huang, X., Zhang, K., Deng, M., Exterkate, R. A. M., Liu, C., Zhou, X., Cheng, L., & Ten Cate, J. M. (2017). Effect of arginine on the growth and biofilm formation of oral bacteria. *Archives of Oral Biology, 82*, 256–262. https://doi.org/10.1016/j.archoralbio.2017.06.026

Jha, P. K., Dallagi, H., Richard, E., Benezech, T., & Faille, C. (2020). Formation and resistance to cleaning of biofilms at air-liquid-wall interface. Influence of bacterial strain and material. *Food Control, 118*, Article 107384. https://doi.org/10.1016/j.foodcont.2020.107384

Jiang, Y., Gao, F., Xu, X., Ye, K., & Zhou, G. (2011). Changes in the composition of the bacterial flora on tray-packaged pork during chilled storage were analyzed by PCR-DGGE and real-time PCR. *Journal of Food Science, 76*(1), M27–M33. https://doi.org/10.3389/fmicb.2019.00043

Jung, Y.-C., Lee, M.-A., & Lee, K.-H. (2019). Role of flagellin-homologous proteins in biofilm formation by pathogenic *Vibrio* species. *mBio, 10*(4), Article e01793. https://doi.org/10.1128/mBio.01793-19, 19.

Karatan, E., & Watnick, P. (2009). Signals, regulatory networks, and materials that build and break bacterial biofilms. *Microbiology and molecular biology reviews: Microbiology and Molecular Biology Reviews, 73*(2), 310–347. https://doi.org/10.1128/MMBR.00041-08

Khan, F., Jeong, G.-J., Tabassum, N., Mishra, A., & Kim, Y.-M. (2022). Filamentous morphology of bacterial pathogens: Regulatory factors and control strategies. *Applied Microbiology and Biotechnology, 106*(18), 5835–5862. https://doi.org/10.1007/s00253-022-12128-1

Kim, S., Li, X.-H., Hwang, H.-J., & Lee, J.-H. (2020). Thermoregulation of *Pseudomonas aeruginosa* biofilm formation. *Applied and Environmental Microbiology, 86*(22), Article e01584. https://doi.org/10.1128/AEM.01584-20, 20.

Li, X., Nielsen, L., Nolan, C., & Halverson, L. J. (2010). Transient alginate gene expression by *Pseudomonas putida* biofilm residents under water-limiting conditions reflects adaptation to the local environment. *Environmental Microbiology, 12*(6), 1578–1590. https://doi.org/10.1111/j.1462-2920.2010.02186.x

Li, W., Siddique, M. S., Graham, N., & Yu, W. (2022). Influence of temperature on biofilm formation mechanisms using a gravity-driven membrane (GDM) system: Insights from microbial community structures and metabolomics. *Environmental Science & Technology, 56*(12), 8908–8919. https://doi.org/10.1021/acs.est.2c01243

Liu, J., Wu, S., Feng, L., Wu, Y., & Zhu, J. (2023). Extracellular matrix affects mature biofilm and stress resistance of psychrotrophic spoilage *Pseudomonas* at cold temperature. *Food Microbiology, 112*, Article 104214.

Liu, Y. J., Xie, J., Zhao, L. J., Qian, Y. F., Zhao, Y., & Liu, X. (2015). Biofilm Formation characteristics of *Pseudomonas lundensis* isolated from meat. *Journal of Food Science, 80*(12), M2904–M2910. https://doi.org/10.1111/1750-3841.13142

Ma, L., Conover, M., Lu, H., Parsek, M. R., Bayles, K., & Wozniak, D. J. (2009). Assembly and development of the *Pseudomonas aeruginosa* biofilm matrix. *PLoS Pathogens, 5*(3), Article e1000354. https://doi.org/10.1371/journal.ppat.1000354

Mann, E. E., & Wozniak, D. J. (2012). *Pseudomonas* biofilm matrix composition and niche biology. *FEMS Microbiology Reviews, 36*(4), 893–916. https://doi.org/10.1111/j.1574-6976.2011.00322.x

Ni, Y., Hou, Y., Kang, J., & Zhou, M. (2021). ATP-dependent protease ClpP and its subunits ClpA, ClpB, and ClpX involved in the field bismerthiazol resistance in *Xanthomonas oryzae* pv. *Oryzae*. *Phytopathology®, 111*(11), 2030–2040. https://doi.org/10.1094/PHYTO-01-21-0011-R

Or, D., Phutane, S., & Dechesne, A. (2007). Extracellular polymeric substances affecting pore-scale hydrologic conditions for bacterial activity in unsaturated soils. *Vadose Zone Journal, 6*(2), 298–305. https://doi.org/10.2136/vzj2006.0080

Osman, S. F., Fett, W. F., & Fishman, M. L. (1986). Exopolysaccharides of the phytopathogen *Pseudomonas syringae* pv. *glycine*. *Journal of Bacteriology, 166*(1), 66–71. https://doi.org/10.1128/jb.166.1.66-71.1986

Otzen, D., & Nielsen, P. H. (2008). We find them here; we find them there: Functional bacterial amyloid. *Cellular and Molecular Life Sciences: CMLS, 65*(6), 910–927. https://doi.org/10.1007/s00018-007-7404-4

Paz-Méndez, A., Lamas, A., Vázquez, B., Miranda, J., Cepeda, A., & Franco, C. (2017). Effect of food residues in biofilm formation on stainless steel and polystyrene surfaces by *Salmonella enterica* strains isolated from poultry houses. *Foods, 6*(12), 106. https://doi.org/10.3390/foods6120106

Penesyan, A., Paulsen, I. T., Kjelleberg, S., & Gillings, M. R. (2021). Three faces of biofilms: A microbial lifestyle, a nascent multicellular organism, and an incubator for diversity. *Npj Biofilms and Microbiomes, 7*(1), 80. https://doi.org/10.1038/s41522-021-00251-2

Read, R. C., Roberts, P., Munro, N., Rutman, A., Hastie, A., Shryock, T., & Taylor, G. (1992). Effect of *Pseudomonas aeruginosa* rhamnolipids on mucociliary transport and ciliary beating. *Journal of Applied Physiology, 72*(6), 2271–2277. https://doi.org/10.1152/jappl.1992.72.6.2271

Sena-Vélez, M., Redondo, C., Graham, J. H., & Cubero, J. (2016). Presence of extracellular DNA during biofilm formation by *Xanthomonas citri subsp. citri* strains with different host range. *PLoS One, 11*(6), Article e0156695. https://doi.org/10.1371/journal.pone.0156695

Sharma, S., Acharya, J., Banjara, M. R., Ghimire, P., & Singh, A. (2020). Comparison of acridine orange, fluorescent microscopy and gram stain light microscopy for the rapid detection of bacteria in cerebrospinal fluid. *BMC Research Notes, 13*(1), 29. https://doi.org/10.1186/s13104-020-4895-7

Shen, C.-H. (2023). Quantification and analysis of proteins. In *Diagnostic molecular biology* (pp. 231–257). Elsevier. https://doi.org/10.1016/B978-0-323-91788-9.00002-8.

Song, M., Veeranagouda, Y., Ganzorig, M., & Lee, K. (2018). Circular pellicles formed by Pseudomonas alkylphenolica KL28 are a sophisticated architecture principally designed by matrix substance. *Journal of Microbiology, 56*(11), 790–797. https://doi.org/10.1007/s12275-018-8252-7, 2018 Nov.

Spiers, A. J., Bohannon, J., Gehrig, S. M., & Rainey, P. B. (2003). Biofilm formation at the air-liquid interface by the Pseudomonas fluorescens SBW25 wrinkly spreader requires an acetylated form of cellulose. *Molecular Microbiology, 50*(1), 15–27. https://doi.org/10.1046/j.1365-2958.2003.03670.x

Thomas, C., & Tampé, R. (2020). Structural and mechanistic principles of ABC transporters. *Annual Review of Biochemistry, 89*(1), 605–636. https://doi.org/10.1146/annurev-biochem-011520-105201

Wagner, J., Carvajal, A. I., Bracher, A., Beck, F., Wan, W., Bohn, S., Körner, R., Baumeister, W., Fernandez-Busnadiego, R., & Hartl, F. U. (2024). Visualizing chaperonin function in situ by cryo-electron tomography. *Nature, 633*(8029), 459–464. https://doi.org/10.1038/s41586-024-07843-w

Wang, D., Fletcher, G. C., Gagic, D., On, S. L. W., Palmer, J. S., & Flint, S. H. (2023c). Comparative genome identification of accessory genes associated with strong biofilm formation in *Vibrio parahaemolyticus*. *Food Research International, 166*, Article 112605. https://doi.org/10.1016/j.foodres.2023.112605

Wang, D., Fletcher, G. C., On, S. L. W., Palmer, J. S., Gagic, D., & Flint, S. H. (2023a). Biofilm formation, sodium hypochlorite susceptibility and genetic diversity *of Vibrio parahaemolyticus*. *International Journal of Food Microbiology, 385*, Article 110011. https://doi.org/10.1016/j.ijfoodmicro.2022.110011

Wang, S., Zhao, Y., Breslawec, A. P., Liang, T., Deng, Z., Kuperman, L. L., & Yu, Q. (2023b). Strategy to combat biofilms: A focus on biofilm dispersal enzymes. *Npj Biofilms and Microbiomes, 9*(1), 63. https://doi.org/10.1038/s41522-023-00427-y

Wickramasinghe, N. N., Hlaing, M. M., Ravensdale, J. T., Coorey, R., Chandry, P. S., & Dykes, G. A. (2020). Characterization of the biofilm matrix composition of psychrotrophic, meat spoilage pseudomonads. *Scientific Reports, 10*(1), Article 16457. https://doi.org/10.1038/s41598-020-73612-0

Wijman, J. G. E., De Leeuw, P. P. L. A., Moezelaar, R., Zwietering, M. H., & Abee, T. (2007). Air-liquid interface biofilms of *Bacillus cereus*: Formation, sporulation, and dispersion. *Applied and Environmental Microbiology, 73*(5), 1481–1488. https://doi.org/10.1128/AEM.01781-06

Yang, G., Lin, J., Zeng, E. Y., & Zhuang, L. (2019). Extraction and characterization of stratified extracellular polymeric substances in Geobacter biofilms. *Bioresource Technology, 276*, 119–126. https://doi.org/10.1016/j.biortech.2018.12.100